# Ordinary Portland Cement Composites Modified with Recycled Liquid Expanded Polystyrene: Mechanical, Thermal and Water Resistance Properties

Teewara Suwan<sup>1,2,4,\*</sup>, Mizi Fan<sup>3</sup>, Piyapong Wongmatar<sup>1,2</sup>, Chotiros Boonpeng<sup>2</sup> and Peerapong Jitsangiam<sup>4,5</sup>

<sup>1</sup>Excellence Center in Infrastructure Technology and Transportation Engineering, Department of Civil Engineering, Chiang Mai University, Chiang Mai 50200, Thailand

<sup>2</sup>Department of Civil Engineering, Faculty of Engineering, Chiang Mai University, Chiang Mai, 50200, Thailand

<sup>3</sup>Department of Civil and Environmental Engineering, College of Engineering, Design and Physical Sciences, Brunel University, Uxbridge, London, UB8 3PH, UK

<sup>4</sup>Chiang Mai University Advanced Railway Civil and Foundation Engineering Center, Department of Civil Engineering, Faculty of Engineering, Chiang Mai University, Chiang Mai, 50200, Thailand

<sup>5</sup>Multidisciplinary Research Institute, Chiang Mai University, Chiang Mai 50200, Thailand

\*Corresponding author

#### **Abstract:**

This study explores the incorporation of Liquid Expanded Polystyrene (L-EPS) into ordinary Portland cement (OPC) composites as a sustainable route to enhance thermal and durability performance. L-EPS was synthesized using an acetone–toluene solvent system and introduced at 10–20 wt.% replacement. The modified composites exhibited marked functional improvements: thermal conductivity (K) decreased by 20–30% compared with control specimens, while the water permeability coefficient (k) was reduced by up to 87%. Importantly, compressive strength after 28 days remained above 25 MPa, confirming their suitability for non-load-bearing structural applications. These enhancements are attributed to the void-filling and film-forming effects of L-EPS within the cement matrix. However, the incorporation of L-EPS also led to a consistent reduction in compressive and flexural strengths relative to the control mix, indicating a trade-off between functional gains and structural capacity. The findings demonstrate that L-EPS-modified OPC composites combine adequate strength with improved insulation and water resistance, making them promising candidates for partition walls, ceiling boards, renders, and façade elements, particularly in hot-humid climates where energy efficiency and moisture protection are critical.

**Keywords:** Waste expanded polystyrene; Liquid polymer additive; OPC composite; Thermal insulation; Water permeability.

## **Highlights:**

- EPS foam was liquefied (L-EPS) and used as a polymer additive for OPC pastes.
- Thermal conductivity decreased by ~30%; water permeability coefficient fell by up to 87%.
- Compressive/flexural strengths reduced; deflection improved at 15% L-EPS (tradeoff).
- L-EPS valorizes EPS waste and enables moderate insulation for non-load-bearing uses.

#### 1. Introduction

In today's construction industry, modern materials offer a diverse range of options tailored to meet specific purposes and budgets, covering core structures, engineering systems, and architectural finishes. Choosing the right materials can enhance efficiency and sustainability, aligning with current trends in energy conservation and environmental stewardship. Modifying or improving existing materials is often necessary to achieve performance, cost-effectiveness, and environmental goals [1].

# 1.1 Ordinary Portland Cement (OPC) and Cement Additives

OPC is one of the most widely used materials for producing concrete in key structures such as buildings, roads, and bridges. When OPC mixes with water, it undergoes a hydration reaction that forms calcium silicate hydrate (C-S-H), lending strength, durability and resistance to expansion [2]. Although alternative cementitious materials like alkali-activated cement or geopolymer cement have been widely investigated as replacements for OPC to reduce the environmental impacts of OPC production, OPC remains one of the most essential materials in the construction industry today [3-5]. However, to expand the specific properties and capabilities of cement and concrete, certain fresh or hardened properties of OPC require enhancement, such as cement additives.

In practice, cement additives adhere to American Society for Testing and Materials (ASTM) standards, which establish a global framework for efficient selection and consistent material quality [6]. Cement additives, classified by ASTM C494 standards, are categorized for fresh cement and concrete into types: Type A (Water-reducing), Type B (Retarding), Type C (Accelerating), Type D (Water-reducing and retarding), Type E (Water-reducing and accelerating), Type F (Superplasticizer), and Type G (Superplasticizer with retarding properties). Other critical categories include air-entraining agents (ASTM C260) and mineral additives like fly ash, slag, and silica fume, each with specific ASTM standards (C618, C989, C1240) [6,7]. Cement additives, particularly polymers and plastics, are also used to improve OPC's flexibility, reduce cracking, mitigate alkali-silica reaction (ASR), and enhance insulation and water resistance. These additives fall under the category of *miscellaneous additives*. Well-known waterproofing polymers include Acrylic Polymer, Polyurethane (PU), Epoxy Resin, and also Styrene-Butadiene Rubber (SBR) [8-10].

## 1.2 Expanded Polystyrene (EPS) and Resin Identification Coding System (RIC)

In terms of utilizing recycled plastic waste, the integration of recycled EPS foam into cement as a liquid polymer additive is a resource-efficient method that reduces plastic waste and promotes sustainable construction with improved insulation and water-resistant properties. Moreover, EPS foam can help reduce CO<sub>2</sub> emissions during disposal processes like burning or landfilling. As EPS recycling remains limited, global efforts, including Thailand's 2018-2030 strategic plan, aim to reduce single-use plastics and promote recycling [11,12].

In general, plastics are classified into seven main types by the ASTM D7611 International Resin Identification Coding System (RIC). Common plastics include Polyethylene Terephthalate (PET-1), High-density Polyethylene (HDPE-2), Polyvinyl Chloride (PVC-3), Low-density Polyethylene (LDPE-4), Polypropylene (PP-5), Polystyrene (PS-6), and other plastics (7), each suited for specific applications. PET and HDPE are typically used for beverage and food packaging, while LDPE, PP, and PS are used for flexible packaging [13]. EPS, a type of PS, is produced by polymerizing styrene monomers, forming a thermoplastic that expands into a foam containing up to 98% air [14]. Recycling EPS is challenging due to its low density and large volume, while improper incineration can release toxic gases. Therefore, many countries compress EPS for disposal or repurpose it as low-grade products instead of incineration or landfilling [12,14,15].

# 1.3 Novelty and Research Approach

In the construction industry, EPS is widely used as a lightweight aggregate or insulation material in applications such as insulating concrete forms (ICFs), structural insulated panels (SIPs), and even in engineering or architectural designs. This is due to its lightweight properties, good thermal resistance, and cost-effectiveness [16]. A new technique involves using suitable solvents to revert EPS to a liquid plastic state at room temperature. This liquid plastic can then be added to fresh cement or concrete as a polymer-based additive, avoiding the need for incineration and landfilling. By incorporating EPS into the cement matrix, this method retains its waterproofing and flexibility properties, enabling its reuse as a binding material in applications such as thermal insulation, lightweight concrete, or plaster composites in construction [17-20].

As EPS foam is made of polystyrene, a polymer with a primarily non-polar molecular structure, it dissolves in non-polar or slightly polar organic solvents such as acetone, toluene, benzene, or ethyl acetate [20,21]. These solvents can interact with and penetrate the polystyrene chains, breaking the weak van der Waals forces that hold the polymer together. Many studies have investigated various solvents for dissolving EPS foam, including biodiesel [21], n-butyl acetate (n-BA), tetrahydrofuran, methyl ethyl ketone, or carbon tetrachloride [22]. However, through an intensive literature review, a blend of acetone and toluene has been identified as the

most suitable solvent due to its global availability, low viscosity, rapid polystyrene dissolution, and quick evaporation, which optimizes EPS dissolution properties [23,24]. Therefore, a combination of acetone and toluene was used in this study. Additionally, it was also observed that the optimal percentage of L-EPS admixture in OPC paste ranges from 5% to 20% by mass fraction [25,26]. Hence, as discussed earlier, the development of cement-based construction materials with added additives enhances properties such as thermal insulation, water resistance, and reduces environmental impact. Notably, incorporating recycled materials like EPS foam plastic waste into cement helps decrease residual plastic waste in the environment and reduces toxic gas emissions during its disposal.

In recent years, polymer-modified cement composites incorporating recycled plastics have attracted increasing attention for their potential to improve durability, impermeability, and functional properties while simultaneously addressing waste management challenges. For instance, recycled PET have been shown to enhance crack resistance and impact toughness, whereas recycled HDPE improve freeze—thaw durability [27]. Common polymer additives such as styrene—butadiene rubber (SBR) and acrylic emulsions (SAE) have also been investigated in comparative studies of polymer-modified cement [28,29]. However, limited research has explored the incorporation of L-EPS, particularly with regard to its influence on thermal conductivity and water permeability in OPC systems.

In the present work, the environmental benefits are supported indirectly through several measurable aspects of life-cycle assessment (LCA): (i) the diversion of EPS foam waste from landfilling and incineration, which reduces associated greenhouse gas emissions and toxic byproducts [12,30]; and (ii) the demonstrated improvements in thermal insulation, which translate into reduced operational energy demand in buildings, particularly in tropical climates. These benefits are consistent with published findings that highlight the dual advantages of polymer-modified cementitious composites in reducing embodied waste and improving operational efficiency [19,31,32].

The quantified environmental benefits of this green innovation lie in the incorporation of L-EPS, which diverts post-consumer EPS from landfills or incineration and aligns with circular economy principles [12]. Given the density of EPS (~20 kg/m³), each cubic metre of L-EPS mortar at a 15% dosage reuses approximately 9 kg of EPS, equivalent to ~0.45 m³ of packaging waste. This substitution also displaces a portion of OPC volume, which carries an embodied carbon footprint of ~0.85 t CO<sub>2</sub>/t cement, leading to an estimated saving of 30–50 kg CO<sub>2</sub> per m³ of mortar [33]. Such quantified benefits reinforce the claim of green innovation and provide a foundation for future full LCA studies.

Recent studies on polymer-modified cement have highlighted a growing shift towards bio-based and waste-derived polymers; however, very few have examined solvent-dissolved recycled EPS as a functional additive. Unlike previous EPS recycling methods that mainly focused on pelletized or diluted EPS in plaster composites [19,25], this study employs a solvent-based liquid EPS system. It uniquely evaluates the integrated effects on permeability, thermal conductivity, and microstructural characteristics within a single OPC system. This research addresses that gap by investigating the effects of L-EPS on the combined mechanical, thermal, and permeability performance of cement composites, while linking these results to microstructural evidence and benchmarking them against industry-relevant performance standards. This approach represents an alternative pathway to promoting sustainability in the construction industry, in alignment with long-term sustainable development goals.

# 2. Experimental programme

#### 2.1 Materials

OPC Type 1, a general-purpose cement conforming to ASTM C150, was used in this study with a specific gravity of 3.14. Recycled EPS foam, a waste polymer-based additive prime material, was collected through a waste recycling campaign involving the university and local communities. Most of the EPS originated from packaging materials for electrical equipment such as screens, computers, and air conditioners (Figure 1a). An acetone–toluene solvent blend, mixed at a 2:1 mass ratio, was employed to dissolve shredded EPS foam into a viscous liquid polymer (L-EPS). This selection was based on its rapid dissolution rate, low viscosity, and prior evidence of compatibility with cementitious systems. The acetone, an analytical reagent grade from RCI Labscan, had a purity of 99%, a specific gravity of 0.788, a melting point of -94 °C, and a boiling point of 56.6 °C. Similarly, analytical reagent grade toluene from the same brand was used, with a purity of 99%, a specific gravity of 0.868, a melting point of -95 °C, and a boiling point of 110.6 °C (Figure 1b).









Figure 1a. Recycled Expanded Polystyrene (EPS)

Figure 1b. Acetone and toluene solvents

**Figure 1** EPS foam from waste collection campaign and Analytical grade solvents.

# 2.2 Mix proportions

The reference OPC paste was prepared with a water-to-cement (w/c) ratio of 0.40. To generate the L-EPS additive, acetone (A) and toluene (T) were blended at a mass ratio of 2:1, forming the combined solvent (S). Shredded waste EPS foam, cut to ≤5 cm in size, was then introduced at an EPS-to-solvent mass ratio of 1:1.5. The acetone–toluene mixture was premixed at ambient temperature (~28 ± 2 °C), after which the EPS was gradually incorporated. Complete dissolution occurred within approximately 30–45 seconds, producing a homogeneous and viscous L-EPS resin. All procedures were carried out under safety precautions, including the use of a well-ventilated area and strict avoidance of ignition sources due to the flammable nature of the solvents. The step-by-step process of L-EPS preparation is illustrated in Figure 2. To investigate the effect of the presence of L-EPS in the OPC paste, its mass was varied from 0% (control mix) to 10%, 15%, and 20% of the OPC paste mass.

Please note that pilot tests were conducted by the authors prior to the full experimental program. The results indicated that the appropriate range of L-EPS incorporation lies between 10–20%. Our preliminary screening showed that additions below 10% provided only marginal improvements, whereas contents above 20% resulted in excessive loss of compressive strength and workability issues, consistent with observations reported for polymer-modified mortars [34]. The selected range therefore represents the most promising balance between functional benefits and structural performance. Moreover, these dosage levels were chosen based on prior optimization studies on polymer–cement systems, which identified 10–20% EPS resin addition as optimal for balancing mechanical performance with permeability reduction, while achieving improved ductility at approximately 15% [35,36].

First, the OPC paste was initially mixed in a 5-liter mortar mixer for 90 seconds at 140  $\pm$  5 rpm at a room temperature of 28  $\pm$  2 °C. After that, the prepared L-EPS was added to the mixer and mixed for another 90 seconds. After thorough mixing, the fresh L-EPS-modified

OPC paste was cast into  $40 \times 40 \times 160$  mm prism moulds (EN 196-1) and immediately wrapped with plastic sheeting to prevent moisture loss. After 24 hours, the samples were demolded and rewrapped in plastic sheeting. They were then cured at a constant room temperature of  $28 \pm 2^{\circ}$ C in a sealed environment until reaching the standard testing ages of 7 and 28 days. A total of four cement paste mixes were prepared, and their specific proportions are presented in Table 1.

Table 1 Mix proportions for L-EPS-modified OPC pastes.

Mix ID	OPC: L-EPS	OPC (%)	L-EPS (%)	w/c ratio	EPS:S
Control OPC	100:0	100	0	0.40	-
EPSC10	90:10	90	10	0.40	1:1.5
EPSC15	85:15	85	15	0.40	1:1.5
EPSC20	80:20	80	20	0.40	1:1.5

Note: EPSC10 refers to a mixture containing 90% OPC paste and 10% liquid EPS additive by mass.

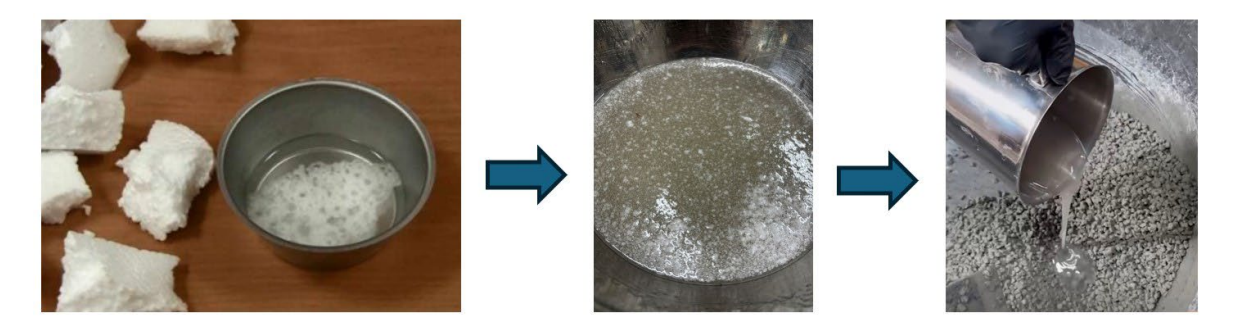


Figure 2 Dissolution of EPS foam in a solvent to form liquid EPS (L-EPS) additive.

## 2.3 Analytical Methods

All mixtures complied with ASTM C191 and ASTM C1437 standards for setting time and flowability. Flexural and compressive strengths were evaluated on  $40 \times 40 \times 160$  mm specimens. A minimum of 3 and 6 samples were tested for each mix, respectively, using a 250 kN Controls universal testing machine.

X-ray diffraction (XRD) was conducted using a 4-circle kappa goniometer diffractometer with a microfocus sealed tube (Mo) and direct photon-counting detector (HyPix-Bantam) to investigate crystalline composition within the 10-60° 2θ range. Fourier Transform Infrared (FTIR, Thermo Nicolet 6700) spectroscopy with attenuated total reflectance (ATR) was used to identify functional groups within the spectral range of 400-4,000 cm<sup>-1</sup>. Scanning electron microscopy (SEM, JEOL JSM-5910LV) was used at 30 kV in vacuum mode to observe microstructure.

For thermal analysis, a Differential Scanning Calorimetry (DSC) Mettler-Toledo, DSC1 model was primarily used to observe heat flow and enthalpy changes in the cement mixes, a temperature range of 25°C to 550°C was applied at a heating rate of 10°C per minute. Thermogravimetric Analysis (TGA) Rigaku, Thermo Plus Evo23 was used to observe mass change and thermal degradation within a temperature range of 25°C to 800°C. Additionally, thermal conductivity (*K*; W/m-K) was measured using a Guarded-Hot-Plate Apparatus, HFM300, within a temperature range of 10°C to 50°C for steady-state heat flux measurements and thermal transmission properties. The sample size for thermal conductivity measurement was 300 mm × 300 mm × 15 mm in accordance with ASTM C177-13 (Figure 3).



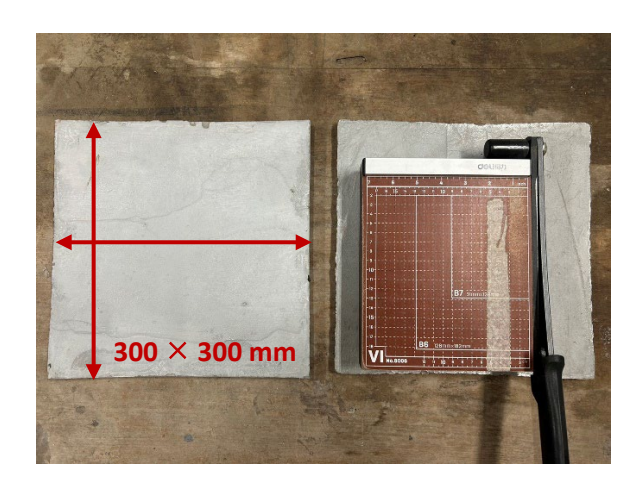


Figure 3a. Guarded-Hot-Plate Apparatus

Figure 3b. Test Sample

Figure 3 thermal conductivity measurement.

Water permeability testing was conducted on samples using an 8-cell MD-C131 apparatus. Cylindrical specimens with a diameter of 50 mm and a depth of 25 mm were subjected to controlled water pressure. The water permeability, measured in meters per second (m/s), was determined to assess the permeability of the cement-based materials. This testing methodology aligns with the guidelines provided by the American Concrete Institute (ACI) (Figure 4).



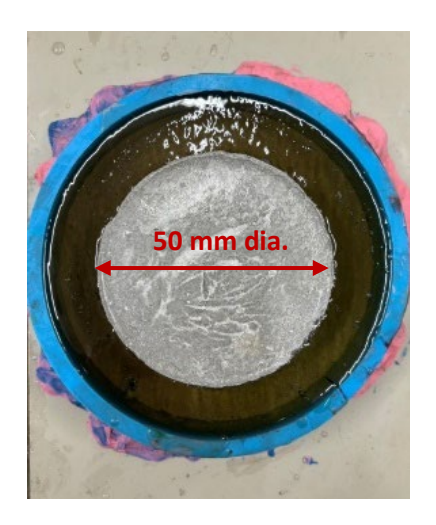


Figure 4a. An 8-Cell MD-C131 apparatus and test specimens set up

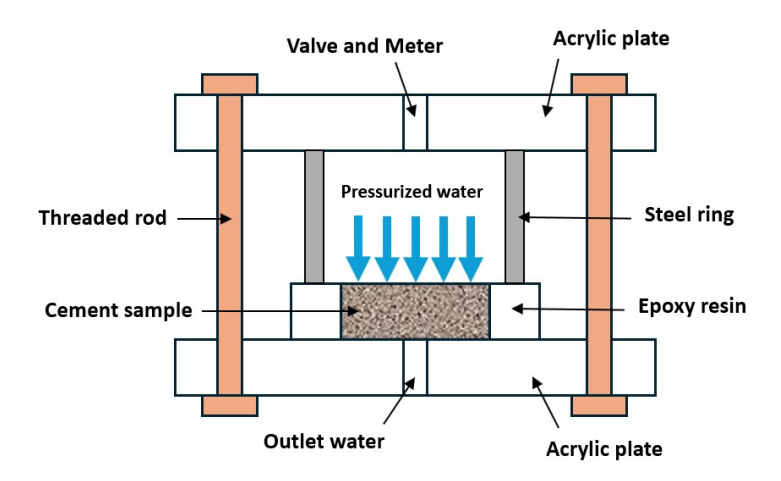


Figure 4b. Schematic diagram of the testing apparatus

Figure 4 Water permeability testing.

#### 3. Results and discussion

# 3.1 Physical and Mechanical properties

It is noted that the flowability of all pastes was maintained within the normal flow range of 100% to 120% in accordance with ASTM C1437 for consistency. The unit weight of the pastes at 28 days was found to decrease as the proportion of L-EPS increased to 10%, 15%, and 20% by weight. As shown in Figure 5, the unit weight of the specimen without added L-EPS (Control OPC) was the highest, at 1,865.8 kg/m³. When the proportion of L-EPS was increased to 10% (EPSC10), the unit weight dropped to 1,779.8 kg/m³, and it decreased further as the proportion increased to 15% (EPSC15) and 20% (EPSC20), with unit weights of 1,618.4 kg/m³ and 1,576.5 kg/m³, respectively. The test results demonstrate that as the proportion of L-EPS increases, the unit weight decreases. This trend is attributed to the lower density of L-EPS

compared to cement, as well as the dispersion of air bubbles, which further reduces the weight of the resulting materials.

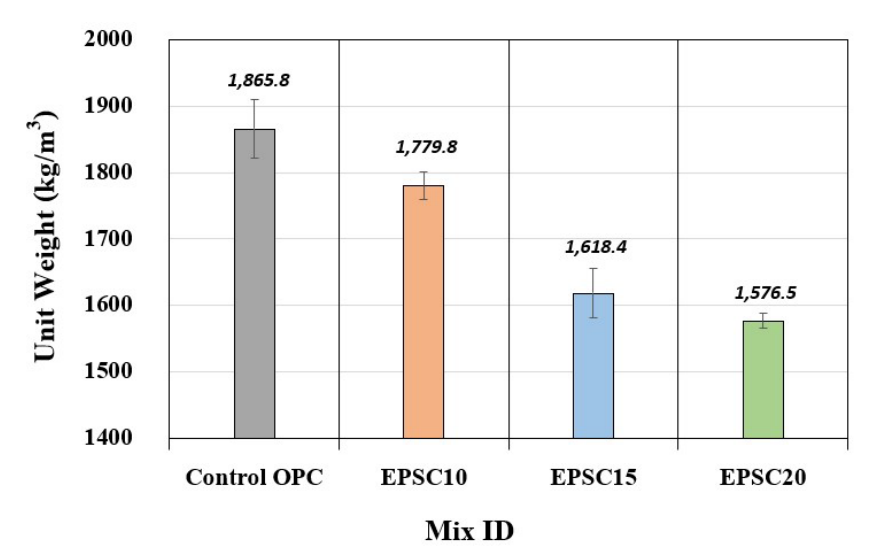


Figure 5 Unit weight of the control mix and with added L-EPS.

The compressive strength of L-EPS—modified OPC paste mixes was evaluated with the L-EPS contents of 0%, 10%, 15%, and 20% by weight. The results demonstrate a clear decline in compressive strength as the proportion of L-EPS increases. At 7 days of curing, the compressive strengths were 32.49 MPa, 14.75 MPa, 9.39 MPa, and 5.14 MPa for the Control OPC, EPSC10, EPSC15, and EPSC20, respectively. After 28 days of curing, the compressive strengths significantly improved across all mixes, with values of 45.69 MPa, 38.71 MPa, 29.82 MPa, and 26.49 MPa for the respective L-EPS contents. As illustrated in Figure 6, the results indicate a consistent reduction in compressive strength with increasing L-EPS content for both 7-day and 28-day curing periods. This reduction is attributed to the lower density and weaker mechanical properties of L-EPS, which dilute the cementitious matrix. However, the strength gain observed at 28 days highlights the continued hydration and improved bonding over time. The observed trends align with the corresponding reduction in unit weight caused by higher L-EPS content, emphasizing the trade-off between strength and weight reduction in these mixes.

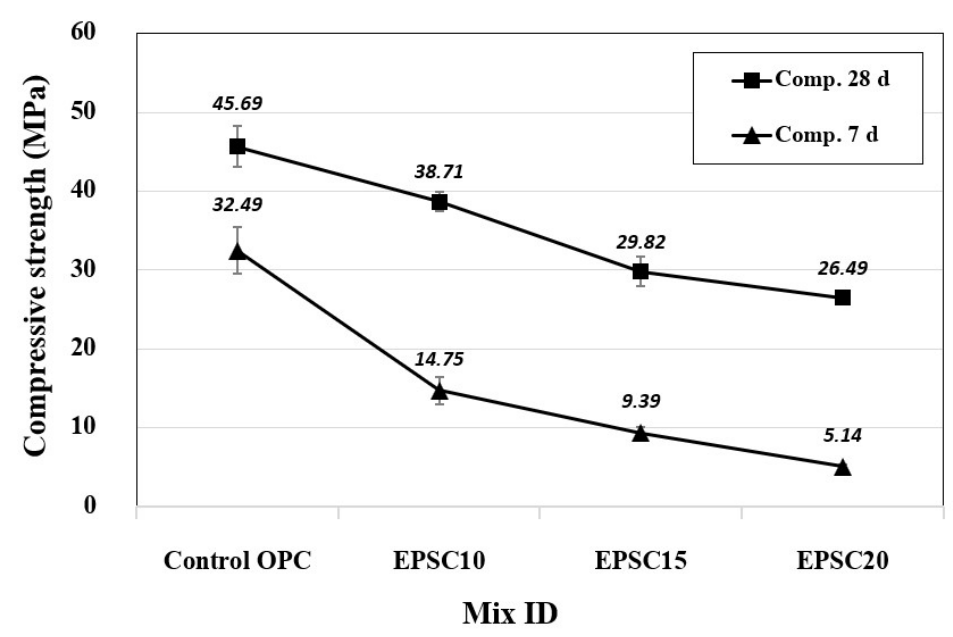


Figure 6 Compressive strength of the control mix and with added L-EPS.

The flexural strength of L-EPS—modified OPC paste mixes was tested using the same L-EPS contents as the compression tests. At 7 days of curing, the flexural strength values were 3.21 MPa, 2.34 MPa, 2.83 MPa, and 2.17 MPa, respectively. These values increased after 28 days of curing, reaching 6.29 MPa, 4.08 MPa, 4.33 MPa, and 3.29 MPa, respectively. As illustrated in Figure 7, the trends in flexural strength at both 7 and 28 days exhibit a similar decreasing pattern to the compressive strength as the L-EPS content increased. Incorporating L-EPS into the mixes generally reduced flexural strength compared to the control (0% L-EPS). This can be attributed to the weakening of the L-EPS—modified OPC paste matrix by the low-density foam, which diminishes internal cohesion and load-bearing capacity. At EPSC10, a significant reduction in flexural strength was observed. Interestingly, at EPSC15, the flexural strength showed a slight increase. This may be due to the optimal dispersion of foam particles within the cement matrix, potentially improving load distribution. However, at EPSC20, the flexural strength decreased again, suggesting that excessive foam content compromises the structural integrity of the matrix.

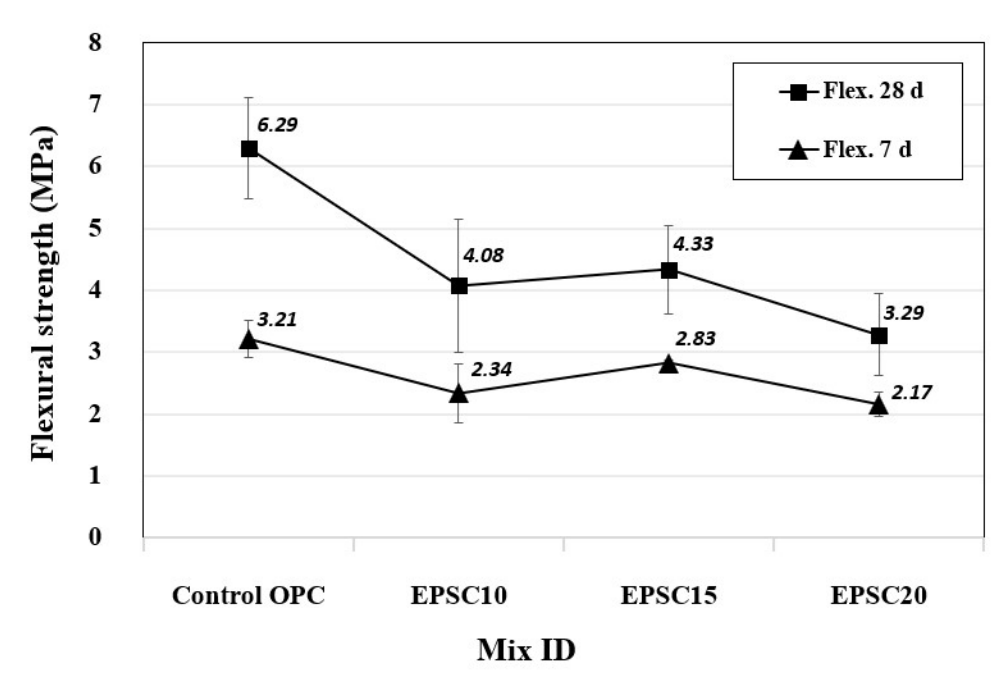


Figure 7 Flexural strength of the control mix and with added L-EPS.

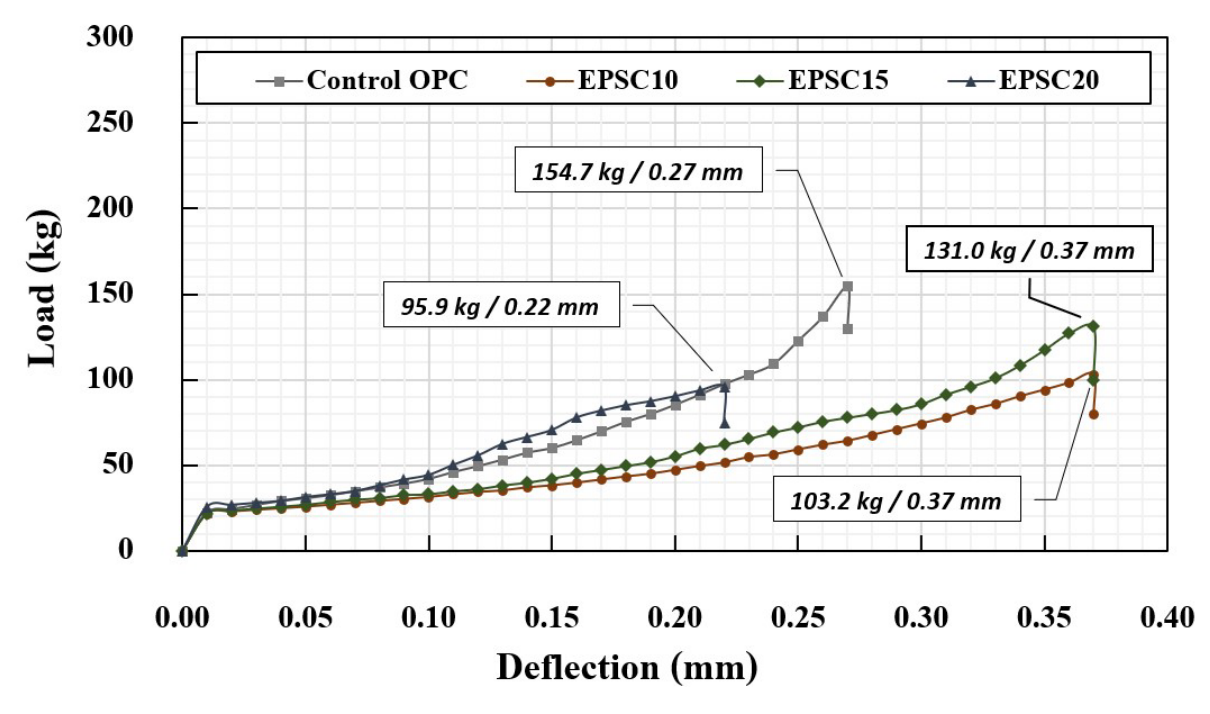
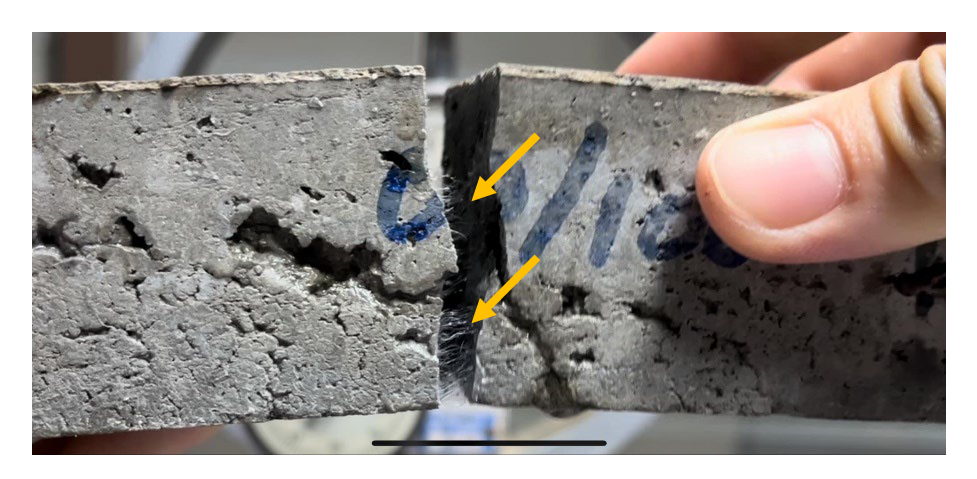


Figure 8 Load-Deflection Behavior of the control mix and with added L-EPS.



**Figure 9**. Crack bridging of L-EPS in a Load-Deflection Test of the EPSC15 mix.

To evaluate the flexibility of L-EPS-modified mixtures, the Load-deflection behavior of the Control OPC and L-EPS-Modified Mixes was analyzed at 7 days of curing, as shown in Figure 8. The results indicate that the Control OPC demonstrated the highest load-bearing capacity of 154.7 kg with a deflection of 0.27 mm. Incorporating L-EPS reduced the maximum load capacity in the following order: EPSC15 (131.0 kg at 0.37 mm), EPSC10 (103.2 kg at 0.37 mm), and EPSC20 (95.9 kg at 0.22 mm). Notably, the EPSC15 mixture exhibited a higher maximum load-bearing capacity compared to EPSC10 and EPSC20, demonstrating its superior structural performance. This behavior is consistent with the flexural strength test results, which also favor the EPSC15 mixture. The improved performance can likely be attributed to the optimized dispersion of L-EPS particles within the cement matrix, which enhances load distribution and contributes to better mechanical stability.

L-EPS offers similar water absorption reduction (20–40%) to conventional modifiers like styrene–butadiene rubber (SBR) and acrylic emulsions (SAE), but with added sustainability benefits. SBR enhances flexural strength (10–20%) and subbase bonding [28], while SAE improves toughness and crack resistance [29]. Unlike virgin polymers, L-EPS reuses waste material, lowers petrochemical demand, and provides superior thermal insulation. Its effective use in subbase soil further supports its role in sustainable construction, making L-EPS a promising alternative that balances mechanical performance with environmental responsibility.

In terms of deflection, both EPSC10 and EPSC15 displayed increased flexibility and ductility with higher deflection values (0.37 mm) compared to the Control OPC (0.27 mm). This indicates that the inclusion of L-EPS enhances the material's ability to deform under load

without failure. Figure 9 highlights the crack-bridging effect observed in the EPSC15 mixture, where the L-EPS particles effectively improve cohesion and crack resistance.

In practical terms, the combination of improved thermal insulation and reduced water permeability offers tangible benefits in hot–humid regions, where moisture ingress and heat gain accelerate material degradation. The hydrophobic film formed by L-EPS, similar to that reported in EPS-based coatings [37], limits capillary absorption and surface condensation, reducing the risks of efflorescence, mould growth, and reinforcement corrosion. Additionally, the 20–30 % reduction in thermal conductivity can lower interior peak temperatures in building envelopes, reducing cooling energy demand, a benefit particularly relevant in tropical climates [35,38]. These combined effects indicate that L-EPS–modified mortars are well-suited for façade renders, lightweight blockwork, and roof screeds in ASEAN conditions.

EPS is chemically stable under normal environmental conditions and can persist for several decades without significant degradation [12]. Its thermal degradation typically initiates at approximately 260 °C, with mass loss accelerating beyond 350 °C due to chain scission and volatilization [36]. When encapsulated within a dense cementitious matrix, oxygen ingress and UV exposure are restricted, thereby reducing oxidative and photo-degradation processes. Consequently, the long-term degradation of L-EPS within cement and concrete matrices is expected to be minimal. Durability data from L-EPS-modified OPC paste confirm this stability, showing negligible changes in compressive strength and water absorption after 180-day wet-dry and freeze-thaw cycles [35,39]. Nevertheless, future studies should incorporate accelerated ageing protocols to provide quantified predictions of performance over extended service lifetimes.

# 3.2 Amorphous phases and functional groups

The phase analysis of composite materials incorporating L-EPS at contents of 0%, 10%, 15%, and 20% by weight was conducted at the standard curing age of 28 days (Figure 10). The results reveal that the addition of L-EPS does not significantly affect the hydration reaction. The XRD patterns of all samples were very similar, as confirmed by the presence of mineral crystals commonly identified in cement paste, including calcite (CaCO<sub>3</sub>) or alite or calcium silicate (Ca<sub>3</sub>SiO<sub>5</sub>), portlandite (Ca(OH)<sub>2</sub>), quartz (SiO<sub>2</sub>), and ettringite. These minerals are critical hydration products of cement and play a significant role in determining the mechanical strength of the composite material. However, the results also indicate a reduction or disappearance of the diffraction peaks corresponding to calcite/calcium silicate product and portlandite in mixtures EPSC15 and EPSC20 at approximately 29.5° and 34.2° (2θ),

respectively. This phenomenon is attributed to L-EPS, which dissolves during the hydration process and forms a film-like structure upon hardening. This film coats the internal surfaces of the composite material, influencing the diffraction of incident and reflected X-rays and thereby preventing the identification of certain crystalline components in the material structure. These findings align with previous observations and are further supported by the following SEM results [36].

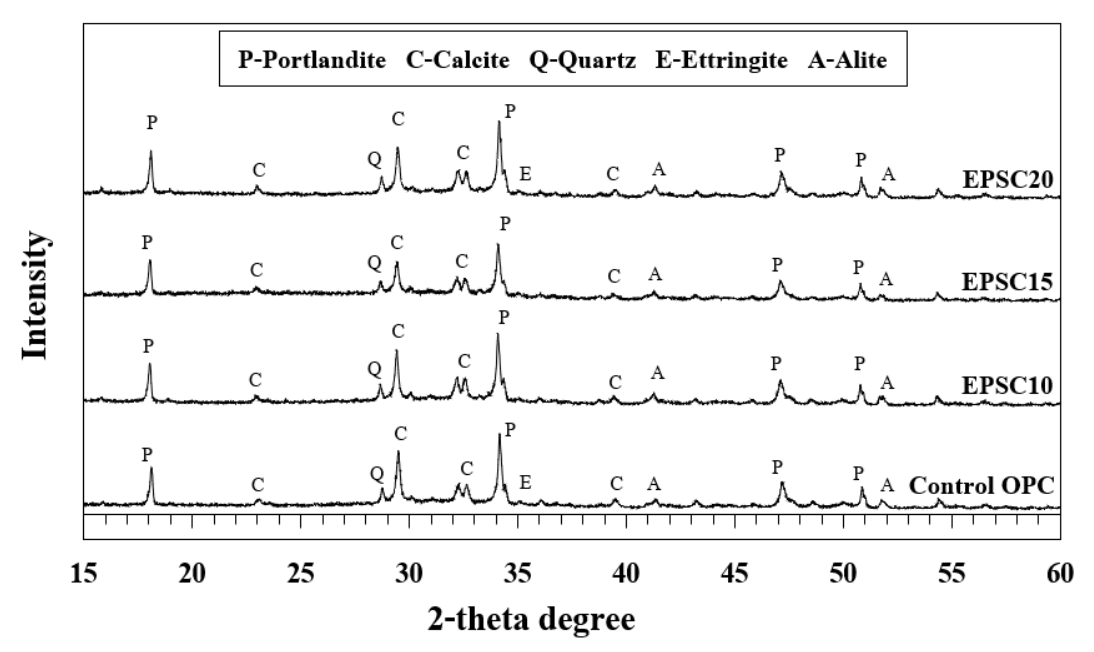


Figure 10 XRD patterns of the control mix and mixtures with added L-EPS.

The spectral patterns from the FTIR analysis of the mixtures are shown in Figure 11. A pronounced peak at 3,640 cm<sup>-1</sup>, corresponding to O-H stretching vibrations of calcium hydroxide (Portlandite), indicates Ca(OH)<sub>2</sub> in all binders. Peaks near 2,840–3,000 cm<sup>-1</sup> and 1,500 cm<sup>-1</sup> reveal alkane C-H and aromatic C=C stretching vibrations, respectively, more prominent in EPSC mixtures due to the dissolved expanded polystyrene foam and residual organic solvents. Peaks near 1,410 cm<sup>-1</sup> and 871 cm<sup>-1</sup>, linked to Si-O and Al-O stretching vibrations in CaCO<sub>3</sub>, diminish with increasing L-EPS content. These reductions correlate with a decline in compressive strength due to reduced formation of calcium-related products. Peaks at 1,110 cm<sup>-1</sup> and 948–966 cm<sup>-1</sup> confirm silica- and alumina-based compounds, particularly calcium silicate hydrate (C-S-H), critical for material strength. A peak near 699 cm<sup>-1</sup>, associated with mono-substituted benzene, originates from expanded polystyrene foam and is absent in the control OPC sample. The incorporation of expanded polystyrene foam dissolved in organic solvents reduces the formation of essential compounds like C-S-H and CaCO<sub>3</sub> without disrupting critical chemical bonds. However, L-EPS replaces the dense cement binder

matrix, leading to lower density and reduced compressive strength, as evidenced by the attenuated vibrational signals and mechanical properties.

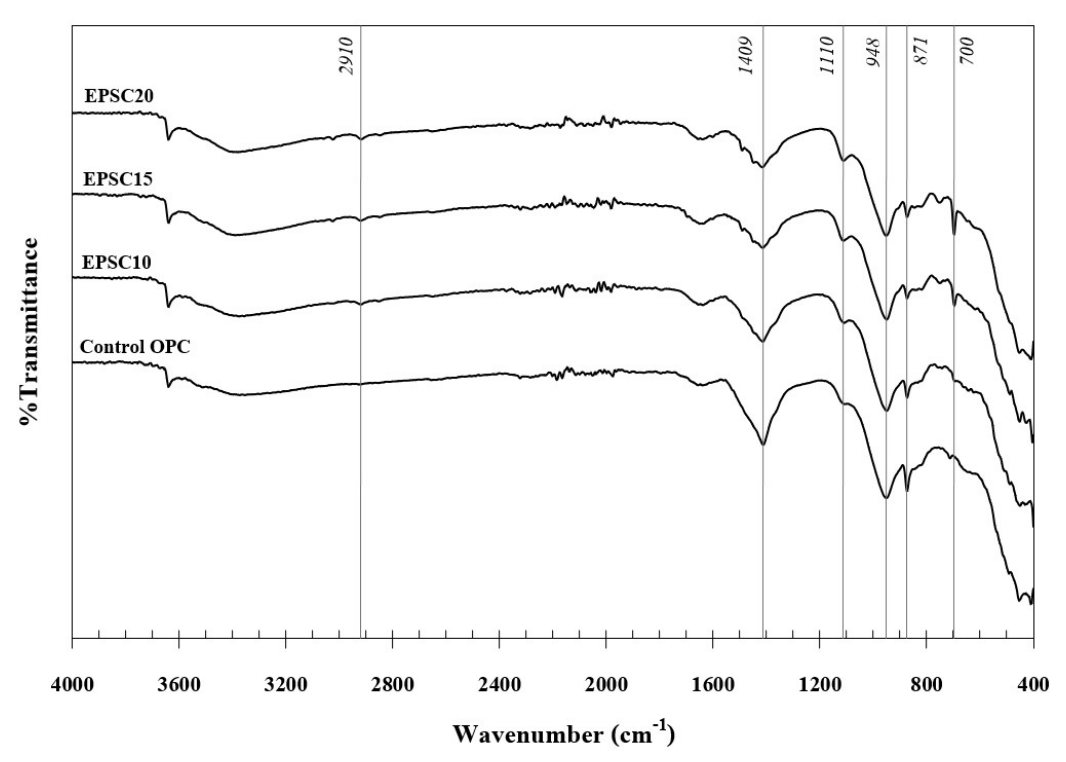


Figure 11 FT-IR analysis of the control mix and mixtures with added L-EPS.

## 3.3 Thermal analysis

# 3.3.1 Thermogravimetric Analysis (TGA)

The results of TGA were used to evaluate the thermal stability of composite materials containing L-EPS. The tests were conducted over a temperature range from ambient room temperature to 800°C, with the percentage of weight loss in different temperature intervals summarized in Table 2. The total weight loss for each sample was as follows: Control OPC exhibited a total weight loss of 26.37%, EPSC10 exhibited a total weight loss of 24.57%, EPSC15 exhibited a total weight loss of 27.45%, and EPSC20 exhibited a total weight loss of 30.53%. The percentage of weight loss varied slightly among the samples, but the data indicates significant weight changes across specific temperature ranges.

A detailed examination of weight loss within these temperature intervals reveals that the initial weight loss (below 150°C) is attributed to the evaporation of free water or physically bound moisture in the L-EPS-modified OPC paste matrix. L-EPS, being a hydrocarbon-based polymer, decomposes in distinct temperature ranges. The major weight loss (approximately 300–400°C) corresponds to the thermal depolymerization of L-EPS, during which polymer chains break down, releasing hydrocarbons and other volatile organic compounds (VOCs).

Additionally, the dehydroxylation of calcium hydroxide (Ca(OH)<sub>2</sub>) was observed in the range of ~450–500°C. At higher temperatures (above 500°C), further decomposition of the cementitious materials occurs. This includes the decarbonation of calcium carbonate, which typically takes place at temperatures exceeding ~700°C.

Table 2

Table 2				
Mixtures	Temperature ranges (°C)	% Mass loss		
	26 - 300 ° C	15.79		
Control OPC	300 - 500° C	3.80		
	500 - 800° C	6.78		
	26 - 800° C	26.37 (Total)		
EPSC10	28 - 300° C	13.58		
	300 - 500° C	4.29		
	500 - 800° C	6.69		
	28 - 800° C	24.57 (Total)		
EPSC15	34 - 300° C	11.89		
	300 - 500° C	7.63		
	500 - 800° C	7.94		
	34 - 800° C	27.45 (Total)		
EPSC20	32 - 300° C	11.57		
	300 - 500° C	10.91		
	500 - 800° C	8.05		
	32 - 800° C	30.53 (Total)		

However, it is evident that the presence of L-EPS in cement mixtures acts as a lightweight filler, and its degradation results in noticeable weight loss on the TGA curve. The significant mass loss of L-EPS in cement, starting around 300–400°C, is typical for polystyrene polymers [16,18]. This is clearly observed in Figure 12, which shows the percentage mass loss of L-EPS between 300°C and 500°C. Specifically, a minimal mass loss of 3.80% was detected in the Control OPC mix, while 4.29%, 7.63%, and 10.91% were observed in EPSC10, EPSC15, and EPSC20, respectively.

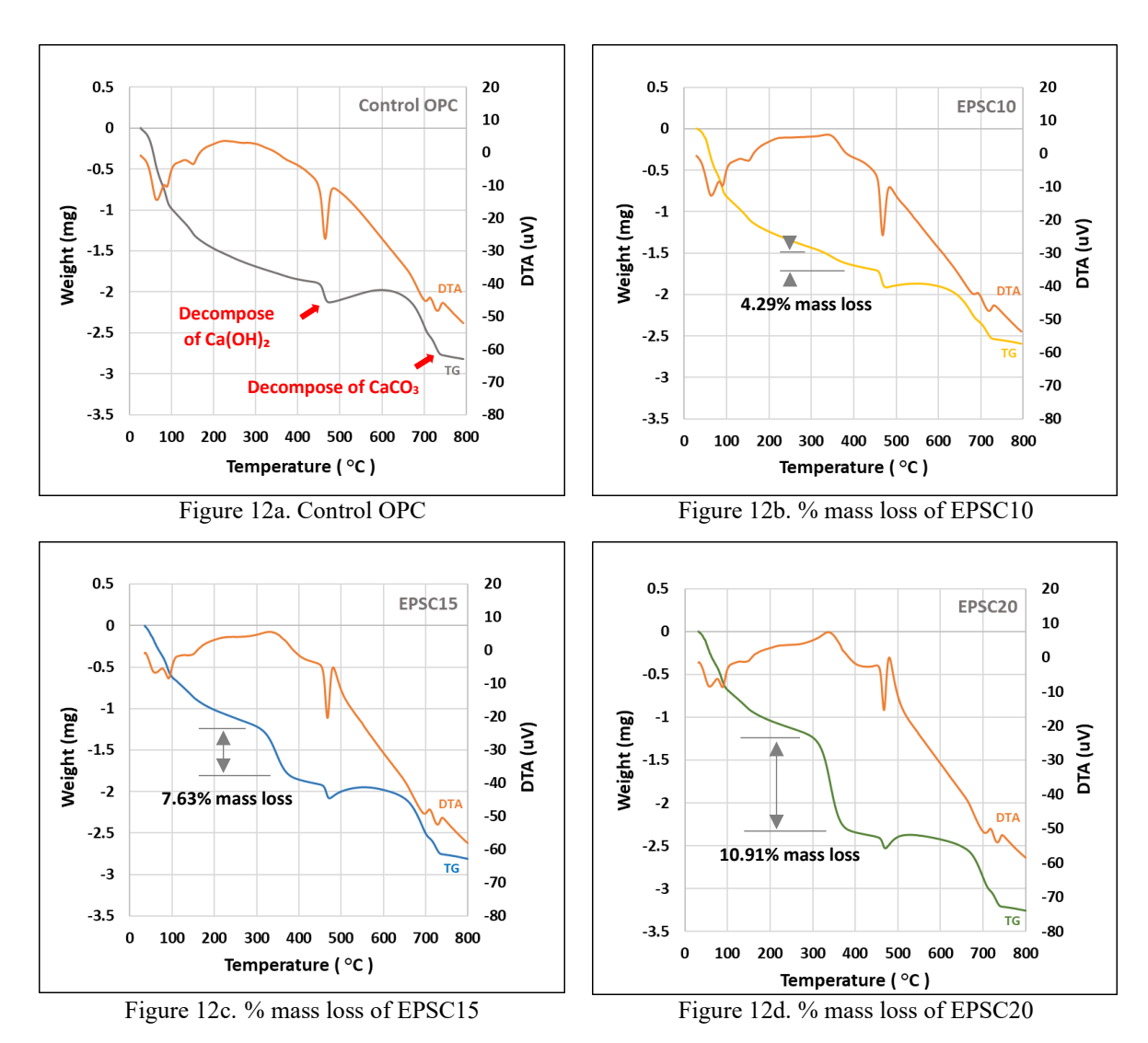


Figure 12 TGA analysis of the control mix and mixtures with added L-EPS.

## 3.3.2 Differential Scanning Calorimetry (DSC)

The DSC analysis measures the heat flow associated with physical or chemical changes in materials as a function of temperature. This study investigates the thermal behavior of control OPC and an EPSC20 for comparison. The heat flow was recorded in millijoules (mJ) as presented in Figure 13.

Figure 13a illustrates the DSC curve of the control OPC mixture. The first peak (at ~100°C) corresponds to the dehydration of physically adsorbed water and water within the pore structure. This includes the loss of free water and some chemically bound water from hydration products such as calcium silicate hydrate (C-S-H) or ettringite. The total energy required for this process was recorded as 2,014.82 mJ. The second peak (at ~180°C) represents the thermal decomposition of calcium silicate hydrate (C-S-H), a primary hydration product of cement paste [40]. The total energy released during this decomposition was measured as 144.53 mJ.

The third peak (at  $\sim 500$ °C) is attributed to the decomposition of calcium hydroxide into calcium oxide (CaO) and water (H<sub>2</sub>O), a key indicator of cement hydration. The total energy associated with this process was recorded as 1,184.64 mJ.

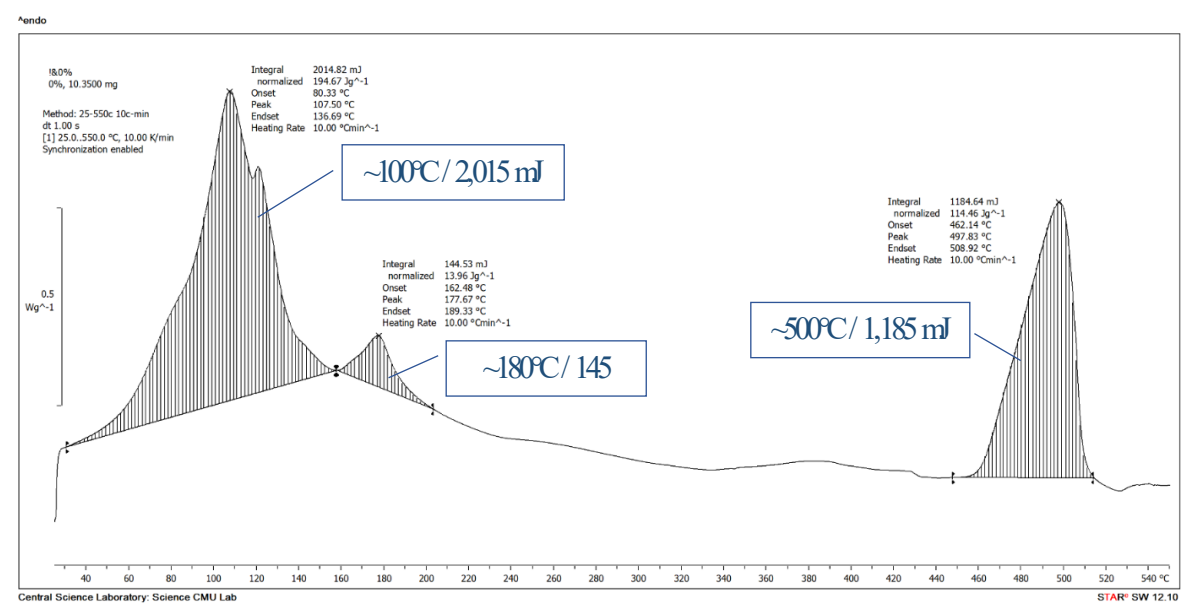


Figure 13a. Control OPC mixture

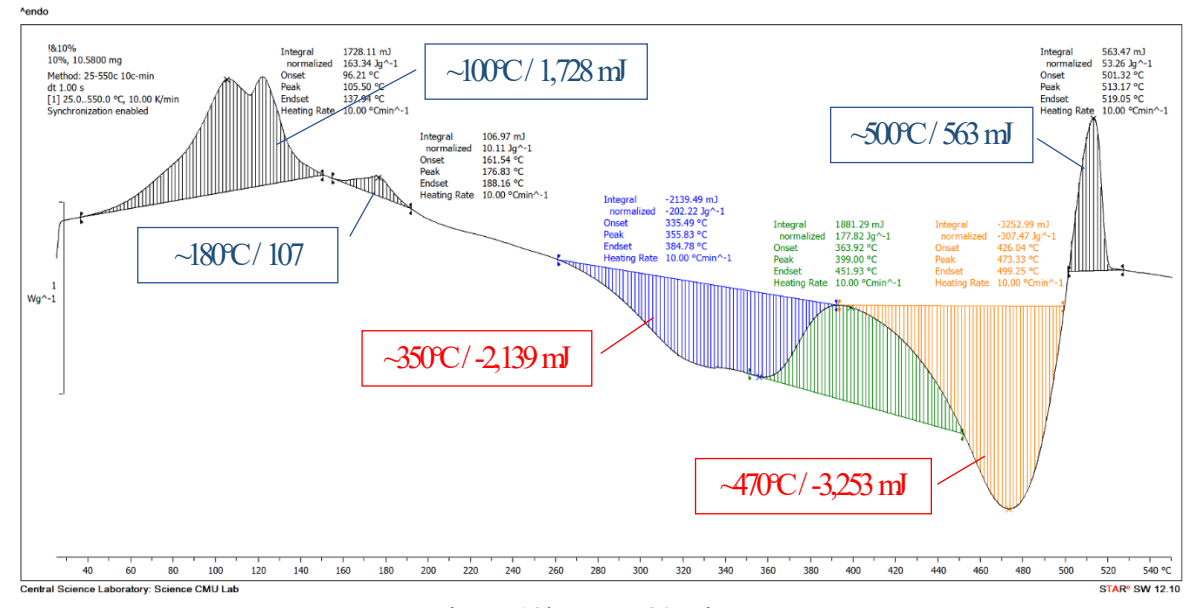


Figure 13b. EPSC20 mixture

Figure 13 DSC analysis of the control OPC and EPSC20 mixtures.

Figure 13b depicts the DSC curve of the EPSC20 mixture. Exothermic peaks at approximately 100°C, 180°C, and 500°C correspond to similar thermal events observed in the control OPC mixture, including the evaporation of free water, the decomposition of calcium silicate hydrate (C-S-H), and the decomposition of calcium hydroxide (Ca(OH)<sub>2</sub>), respectively. However, the total energy integrals for EPSC20 are reduced to 1,728.11 mJ, 106.97 mJ, and

563.47 mJ, indicating lower energy changes compared to the control OPC mixture. A distinct broad endothermic peak is observed between approximately 260°C and 390°C, with an energy change of -2,139.49 mJ. This is likely associated with the thermal decomposition of organic components present in the L-EPS content. As the temperature continues to rise from 400°C to 500°C, another significant endothermic event is observed, with -3,252.99 mJ. This phenomenon may be attributed to the combustion or oxidative degradation of residual EPS foam or carbonaceous materials.

Overall, the combined TGA and DSC results highlight the thermal stability and decomposition behavior of hydration products in the presence of L-EPS additives. Notably, the decomposition of L-EPS significantly affects the thermal behavior within the 300–500°C temperature range, as evidenced by both weight loss and heat flow. Outside this range, the typical cement hydration and decomposition processes predominate. In practical applications, the incorporation of L-EPS in the cement mixture offers beneficial properties, such as enhanced flexibility and water resistance, making it suitable for construction in hot environments or climates with temperatures. At higher temperatures, L-EPS may soften due to its thermoplastic nature, allowing it to regain functional properties when cooled to ambient temperatures. However, since its decomposition begins around 260°C, its use in high-temperature applications, such as fire-resistant structures, may be limited [41].

# 3.3.3 Thermal Conductivity

Thermal conductivity (K) of Control OPC and EPSC20 mixtures was measured between 10 °C and 50 °C using a Guarded-Hot-Plate Apparatus (HFM 300) (Figure 14). EPSC20 consistently exhibited lower thermal conductivity than Control OPC, ranging from 0.1394 to 0.1727 W/m·K, compared to 0.2035 to 0.2454 W/m·K for Control OPC, representing an average reduction of approximately 30%. The 0.14–0.17 W/m·K range observed for L-EPS—modified OPC paste is higher than that of commercial EPS foam (~0.035 W/m·K) and PU foam (~0.025 W/m·K), but falls within the range of lightweight aerated concrete (0.17–0.36 W/m·K), and is comparable to values reported for lightweight geopolymer foam concretes (up to 0.80 W/m·K) and traditional brick walls (0.60–1.0 W/m·K) [27,42]. These results position L-EPS mortar as a viable moderate insulation option, balancing structural compatibility with improved insulation performance, particularly in applications where both durability and thermal efficiency are required.

This is attributed to the L-EPS admixture, which introduces micro-voids and thin films within the L-EPS-modified OPC paste matrix, disrupting heat transfer pathways. Both materials showed a slight increase in thermal conductivity with rising temperature, a typical phenomenon due to enhanced molecular vibrations. However, EPSC20 maintained lower conductivity, demonstrating superior insulation properties. Within the practical building temperature range of 20°C, 30°C, and 40°C, the thermal conductivity reduction was 31.3%, 30.9%, and 30.2%, respectively. This enhanced insulation of L-EPS makes it ideal for energyefficient building materials. However, a trade-off between thermal conductivity and mechanical strength must be considered for specific applications. While the measured thermal conductivity values are encouraging for insulation applications, it is important to note that EPS softens above ~90 °C and undergoes substantial mass loss between 260–500 °C. Accordingly, L-EPS-modified mortars are not intended for use as structural fire-resistant elements without supplementary fire-retardant strategies, such as the incorporation of mineral fillers or intumescent coatings [43]. Nevertheless, under ambient conditions, they provide excellent thermal insulation performance, with the added benefit of recycling EPS waste as a sustainable material resource.

In addition, with regard to acoustic insulation, EPS is well known for its ability to dampen airborne sound, particularly in the mid-high frequency range, owing to its cellular structure and internal energy dissipation [44]. Although acoustic performance was not measured in this study, previous research on L-EPS-modified OPC paste has reported improvements in sound transmission loss [45]. This potential dual functionality—in both thermal and acoustic insulation—merits dedicated investigation in future studies.

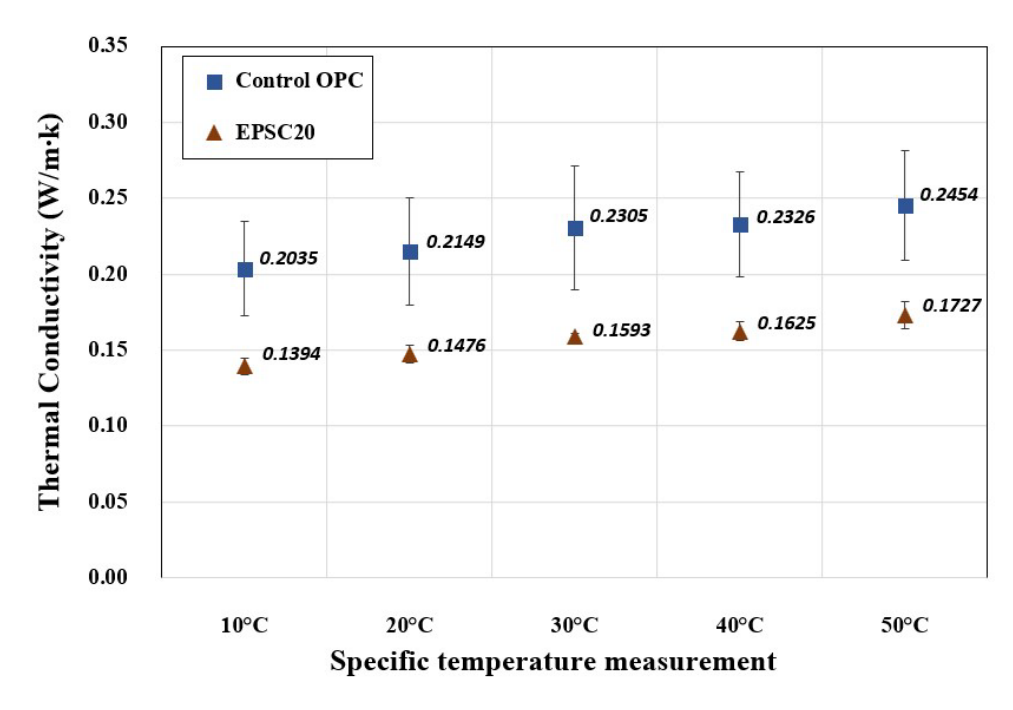


Figure 14 Thermal conductivity of the control OPC and EPSC20 mixtures.

# 3.4 Water permeability

Figure 15 illustrates the water permeability of Control OPC and its mixtures with varying percentages of L-EPS as an additive. The permeability of the Control OPC mix is  $14.81 \times 10^{-8}$  m/s, as typically observed in normal OPC paste, representing the highest value among all samples. Incorporating 10% L-EPS into the mix (EPSC10) reduces the permeability significantly to  $8.77\times10^{-8}$  m/s, demonstrating a reduction of approximately 40.8%. Further increasing the L-EPS content to 15% (EPSC15) results in a permeability of  $4.04\times10^{-8}$  m/s, a reduction of 72.7% compared to the control. The trend continues at 20% L-EPS (EPSC20), where the permeability decreases to  $1.84\times10^{-8}$  m/s, an 87.6% reduction compared to the control.

The consistent decline in water permeability with increasing L-EPS content indicates that L-EPS significantly enhances the material's resistance to water penetration. This improvement can be attributed to the L-EPS particles forming a film-like coating on some cementitious constituents in the matrix and obstructing water pathways. The diminishing reductions in permeability at higher L-EPS contents (e.g., from EPSC15 to EPSC20) suggest diminishing returns, likely due to approaching the optimal threshold for reducing pore connectivity. Lower permeability is a desirable characteristic in cementitious materials, particularly for applications requiring enhanced durability. By reducing permeability, the ingress of aggressive agents, such as water, chlorides, and sulfates, can be minimized, thereby improving resistance to deterioration mechanisms such as corrosion or sulfate attack.

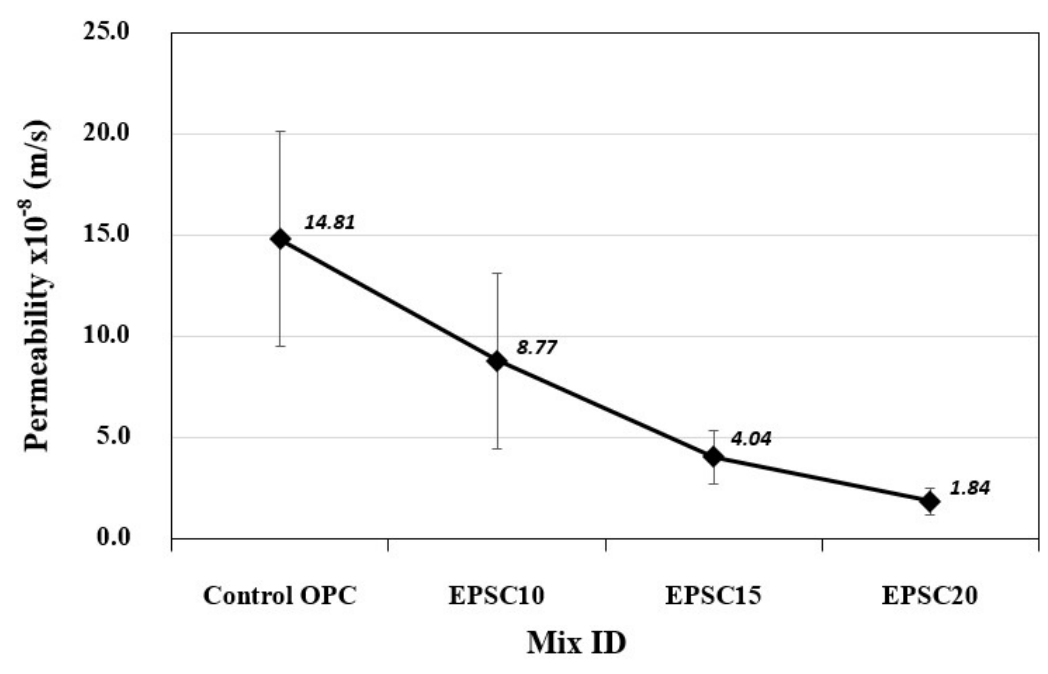


Figure 15 Water permeability of the control mix and with added L-EPS.

# 3.5 Microstructures through SEM Images

The micrographs of the control mix and mixtures with added L-EPS at their standard 28-day curing age are shown in Figures 16a-d. For the control OPC (Figure 16a), typical hydration products of cement, such as calcium silicate hydrate (C-S-H) and ettringite, are prominently observed under high magnification. When 10% and 15% L-EPS were added (EPSC10 and EPSC15, Figures 16b and 16c), the microstructures revealed that the internal morphology of the cement paste still exhibited typical hydration products. The addition of L-EPS did not directly affect the hydration process, as confirmed by the XRD and FTIR test results. However, upon drying, L-EPS exhibited a tendency to bind with certain cementitious products, forming clusters that contributed to reducing pore connectivity.

When the L-EPS content was increased to 20% (EPSC20, Figure 16d), the microstructure still displayed the same hydration products as the control. However, some cementitious products were observed to aggregate into clusters, and a thin film-like coating appeared on the surface of internal cementitious products. In addition to further reducing pore connectivity, the L-EPS particles acted as a film-like barrier within the matrix, obstructing water pathways. These effects contribute to the improved performance of the EPSC mixtures, which achieve excellent thermal insulation properties along with significantly reduced water permeability.

The combined SEM and XRD results provide a clear microstructural explanation for the macroscopic performance enhancements observed in L-EPS-modified composites. SEM

micrographs demonstrate that polymer-rich domains form continuous films and clusters coating hydration products, thereby bridging across pores and disrupting interconnected void networks. This morphology reduces the continuity of capillary channels, directly correlating with the measured 87.6% reduction in water permeability in EPSC20 mixtures. In parallel, XRD analysis confirms that the principal load-bearing crystalline phases, including calcium silicate hydrate (C-S-H) and portlandite, remain unaffected by the presence of L-EPS, indicating that cement hydration proceeds normally. Nevertheless, a reduction in compressive strength is observed, which can be attributed to the lower density of the composite when cement is partially replaced by L-EPS, thereby diminishing its load-bearing resistance. Furthermore, by obstructing fluid pathways and reducing pore connectivity, the polymer films create a more hydrophobic matrix that resists both moisture ingress and ion diffusion, consistent with the enhanced durability reported in accelerated wet-dry and freeze-thaw tests [35,39]. These microstructural modifications also contribute to improved thermal performance, as the polymer domains act as thermal barriers, reducing conductivity by up to 30% and providing more stable thermal profiles under fluctuating external conditions [38]. Collectively, the SEM and XRD evidence highlight the role of L-EPS as a multifunctional additive: it improves impermeability and thermal insulation through microstructural refinement, while preserving the integrity of hydration products essential for long-term performance.

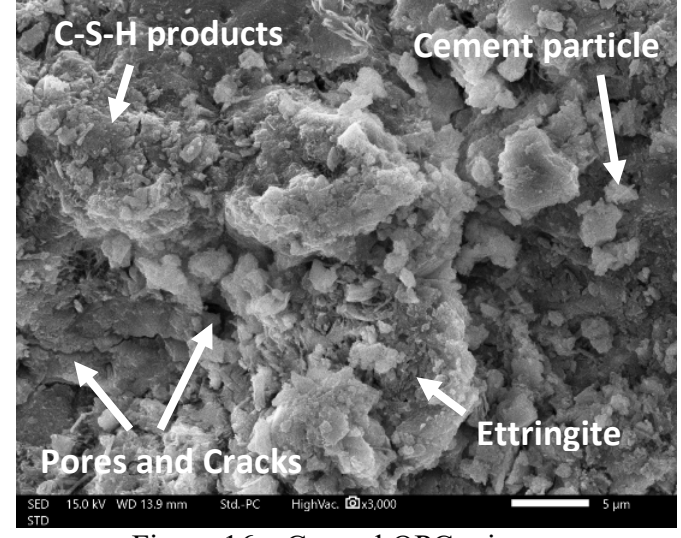


Figure 16a. Control OPC mixture

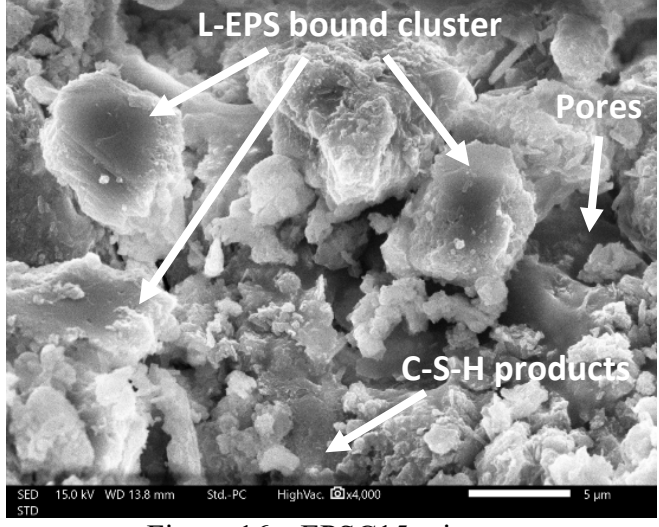


Figure 16c. EPSC15 mixture

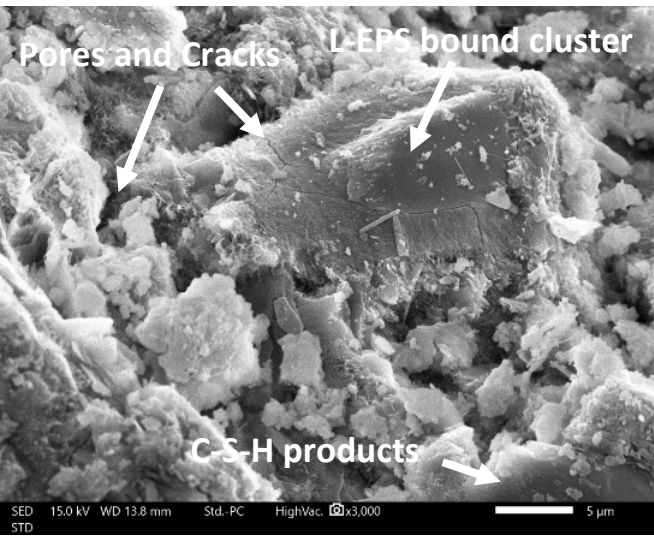


Figure 16b. EPSC10 mixture

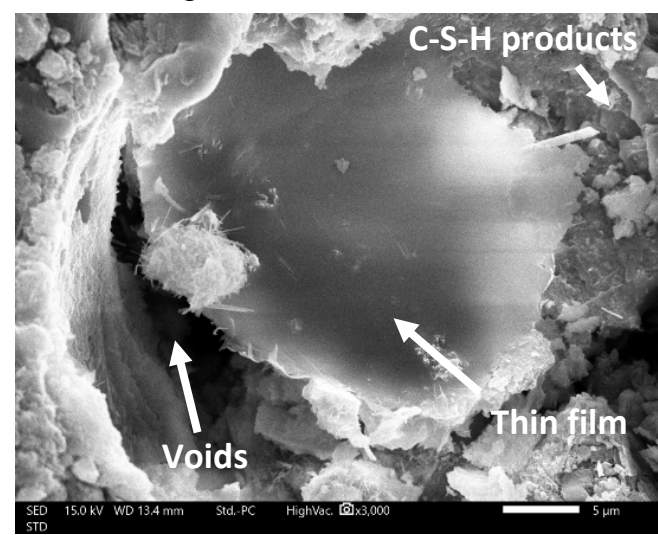


Figure 16d. EPSC20 mixture

Figure 16 Microstructures of the control mix and with added L-EPS.

## 3.6 Practical applications and Standards alignment

To contextualize the findings, the results of L-EPS-modified OPC paste were compared with contemporary work on polymer-modified and recycled plastic-based cement systems. While many studies have focused on durability or mechanical performance individually, limited work has explored integrated thermal, permeability, and acoustic properties in a single system.

The thermal conductivity reduction of approximately 30% achieved in EPSC20 (0.139–0.173 W/m·K) is comparable to PET fibre–reinforced mortars and superior to recycled HDPE-modified concretes (~15% reduction). Although higher than commercial EPS foam (~0.035 W/m·K) or PU foam (~0.025 W/m·K), the values for L-EPS composites align with lightweight aerated concrete (0.17–0.36 W/m·K) and outperforms brick walls (0.60–1.0 W/m·K) [27,42]. This positions L-EPS as a moderate insulation material offering both structural compatibility and sustainability benefits. The water permeability reduction of up to 87.6% surpasses that of SBR-modified mortars (~50%), highlighting the potential of L-EPS to provide improved moisture resistance in humid climates. This property enhances its suitability for ceiling boards, renders, and façade cladding in moisture-prone environments.

The mechanical performance demonstrates compressive strength reductions of 15–42% relative to OPC controls; however, the minimum values (>26 MPa for EPSC20) remain above the ASTM C129 requirement of 3.45 MPa for non-load-bearing units. Flexural strength reductions of 31–48% are also consistent with reported trends in polymer-modified mortars, confirming their appropriateness for non-structural applications. Accordingly, potential applications of L-EPS–modified composites include their use in partition walls and lightweight panels, where they reduce overall building weight while achieving compliance with thermal performance [46]. In ceiling boards and interior renders, the material's reduced capillary absorption—ranging from 50–80%—enhances resistance to condensation and mould growth [47]. For external use, façade renders and cladding benefit from the improved adhesion and rain resistance provided by L-EPS [48]. Additionally, the closed-cell structure of EPS contributes to acoustic insulation performance, delivering airborne sound reduction of 3–5 dB in the mid-frequency range, which is advantageous for noise-reducing internal partitions [49].

Compared with conventional polymer modifiers such as SBR and SAE, L-EPS offers the additional advantage of valorizing plastic waste and reducing virgin polymer consumption, which is significant for scalability and cost efficiency. While performance is comparable in terms of permeability reduction, the environmental and circular-economy benefits uniquely differentiate L-EPS. Collectively, these comparisons highlight the dual functionality of L-EPS

composites—achieving permeability resistance and thermal conductivity reduction while valorizing plastic waste. This differentiates L-EPS from other recycled polymer approaches and underscores its relevance to contemporary sustainable construction practices.

#### 4. Conclusions

This study has demonstrated that incorporating L-EPS into OPC paste provided a feasible approach to improving functional performance while maintaining sufficient mechanical strength. The use of an acetone–toluene solvent system enabled effective dispersion of L-EPS at dosages of 10–20 wt.%, producing composites with distinctive improvements in thermal and durability properties. Thermal conductivity was reduced by 20–30% compared with the control mix, while the water permeability coefficient decreased by up to 87%. Despite these significant enhancements, compressive strength at 28 days remained above 25 MPa, indicating that the material retained adequate load-bearing capacity for non-structural applications. These outcomes highlight the potential of L-EPS modification to deliver lightweight, moisture-resistant, and insulating cement-based composites suitable for partition walls, ceiling boards, façade renders, and acoustic panels. In climates where both energy efficiency and moisture protection are essential, such as hot and humid regions, these composites present tangible benefits over conventional OPC systems.

Nonetheless, the study also identifies some limitations. Fire resistance at elevated temperatures was not investigated, and long-term durability under aggressive wet—dry or freeze—thaw cycles are yet to be determined. The acoustic performance of full-scale components and a comprehensive LCA of embodied carbon were not within the scope of this work. Future research should therefore focus on advanced durability testing, fire performance evaluation, and scaling towards pilot construction projects. Integrating LCA will be essential to quantify the environmental benefits of EPS recycling within cementitious systems. By addressing these aspects, L-EPS—modified OPC paste may evolve into a viable class of sustainable materials that simultaneously enhance energy efficiency, durability, and waste valorization in the construction industry.

# Acknowledgements

This research was partially supported by Chiang Mai University. The authors express their gratitude to the Department of Civil Engineering, Faculty of Engineering, Chiang Mai University, for providing the necessary equipment and facilities. The authors also extend special thanks to Mr. Piroon Siriput (M.Eng.) for his hard work on this project. The authors

- 69 further thank the Science and Technology Park (STeP) at Chiang Mai University (Dr. Win-
- 70 Pitiwat Wattanachai) for their kind support.

# 72 References

71

- [1] Hossain, K. M. A., Anwar, M. S., & Rahman, M. M. (2020). Sustainable lightweight concrete with the use of waste materials and by-products. Construction and Building Materials, 242, 118086.
- [2] Neville, A.M., 2011. Properties of Concrete, Pearson Education Limited. Edinburgh Gate, Harlow England, pp.58-661.
- [3] Bualuang, T., Jitsangiam, P., Suwan, T., Rattanasak, U., Tangchirapat, W. and Thongmunee, S., 2021. Influence of asphalt emulsion inclusion on fly ash/hydrated lime alkali-activated material. Materials, 14(22), p.7017.
- [4] Ramjan, S., Tangchirapat, W., Jaturapitakkul, C., Chee Ban, C., Jitsangiam, P. and Suwan, T., 2021. Influence of cement replacement with fly ash and ground sand with different fineness on alkali-silica reaction of mortar. Materials, 14(6), p.1528.
- [5] Suwan, T., Paphawasit, B., Fan, M., Jitsangiam, P. and Chindaprasirt, P., 2021. Effect of microwave-assisted curing process on strength development and curing duration of cellular lightweight geopolymer mortar. Materials and Manufacturing Processes, 36(9), pp.1040-1048.
- [6] ACI Committee. (2001). Guide for the use of polymer modified concrete. American Concrete Institute.
- [7] Celik, K., Jackson, M.D., Mancio, M., Meral, C., Emwas, A.H., Mehta, P.K. and Monteiro, P.J., 2014. High-volume natural volcanic pozzolan and limestone powder as partial replacements for portland cement in self-compacting and sustainable concrete. Cement and concrete composites, 45, pp.136-147.
- [8] Celik, K., Meral, C., Mancio, M., Mehta, P.K. and Monteiro, P.J., 2014. A comparative study of self-consolidating concretes incorporating high-volume natural pozzolan or high-volume fly ash. Construction and Building materials, 67, pp.14-19.
- [9] Hewlett, P. and Liska, M. eds., 2019. *Lea's chemistry of cement and concrete*. Butterworth-Heinemann.
- [10] Siddique, R., Khatib, J. and Kaur, I., 2008. Use of recycled plastic in concrete: A review. *Waste management*, 28(10), pp.1835-1852.
- [11] Hama, S. M., & Hilal, N. N. (2017). Fresh properties of self-compacting concrete with plastic waste as partial replacement of sand. International Journal of Sustainable Built Environment, 6(2), 299-308.
- [12] Global EPS Sustainability Alliance (GESA). (2024). Expanded Polystyrene Environmental Profile General Version [PDF]. Retrieved from https://globaleps.org/wp-content/uploads/2024/02/gesa-environmental-profile-general-version-feb-2024-edit.pdf
- [13] Andrady, A. L., & Neal, M. A. (2009). Applications and societal benefits of plastics. Philosophical Transactions of the Royal Society B: Biological Sciences, 364(1526), 1977-1984.
- [14] Zhao, W., Zhao, H.B., Cheng, J.B., Li, W., Zhang, J. and Wang, Y.Z., 2022. A green, durable and effective flame-retardant coating for expandable polystyrene foams. Chemical Engineering Journal, 440, p.135807.
- [15] Alleguard (2024) Unveiling the Truth: EPS Recycling Facts and Myths. Available at: https://alleguard.com/insights/unveiling-the-truth-eps-recycling-facts-and-myths/ (Accessed: 29 October 2024).

- [16] Capricho, J.C., Prasad, K., Hameed, N., Nikzad, M., and Salim, N., 2022. Upcycling polystyrene. Polymers, 14(22), p.5010
- [17] Boonpeng, C., Suwan, T., Liu, W., Hansapinyo, C. and Paphawasit, B., 2022, May. Properties of Porous Concrete Using Expanded Polystyrene (EPS) Foam Waste as Cement Binder Admixture. In International Conference on Environment Sciences and Renewable Energy (pp. 75-84). Singapore: Springer Nature Singapore.
- [18] Ramli Sulong, N.H., Mustapa, S.A.S., and Abdul Rashid, M.K., 2019. Application of expanded polystyrene (EPS) in buildings and constructions: A review. Journal of Applied Polymer Science, 136(20), p.47529
- [19] Zaragoza-Benzal, A., Ferrández, D., Atanes-Sánchez, E., and Saíz, P., 2023. Dissolved recycled expanded polystyrene as partial replacement in plaster composites. Journal of Building Engineering, 65, p.105697
- [20] Prasittisopin, L., Termkhajornkit, P. and Kim, Y.H., 2022. Review of concrete with expanded polystyrene (EPS): Performance and environmental aspects. Journal of Cleaner Production, 366, p.132919.
- [21] Chaudhary, A., Dave, M., and Upadhyay, D.S., 2022. Value-added products from waste plastics using dissolution technique. Materials Today: Proceedings, 57, pp.1730-1737
- [22] Uttaravalli, A.N., Dinda, S., Gidla, B.R., Kasturi, G., Kasala, P., and Penta, G., 2021. Studies on development of adhesive material from post-consumer (waste) expanded polystyrene: a two-edged sword approach. Process Safety and Environmental Protection, 145, pp.312-320
- [23] Eskander, S.B. and Tawfik, M.E., 2011. Polymer–cement composite based on recycled expanded polystyrene foam waste. Polymer Composites, 32(9), pp.1430-1438
- [24] Van Deursen, C., Suwan, T., Laosuwan, S., Wongmatar, P., Kaewmoracharoen, M. and Suwan, P., 2023, February. Development of Polymeric Binder from Expanded Polystyrene (EPS) Foam Waste as Construction Materials. In IOP Conference Series: Earth and Environmental Science (Vol. 1146, No. 1, p. 012007). IOP Publishing
- [25] Amariles-López, C.C., Aristizábal-Torres, D., Alzate-Buitrago, A., Osorio-Gómez, C.C. and Mancilla-Rico, E., 2024. Physicomechanical Properties of Mortar with Diluted EPS as the Binding Material. Journal of Materials in Civil Engineering, 36(12), p.04024414.
- [26] El-Sayed, A.M., Faheim, A.A., Salman, A.A. and Saleh, H.M., 2022. Sustainable lightweight concrete made of cement kiln dust and liquefied polystyrene foam improved with other waste additives. Sustainability, 14(22), p.15313.
- [27] Abdellatief, M., Mortagi, M., Hamouda, H., Skrzypkowski, K., Zagórski, K. and Zagórska, A., 2025. Influence of silicate modulus and eggshell powder on the expansion, mechanical properties, and thermal conductivity of lightweight geopolymer foam concrete. Materials, 18(9), p.2088.
- [28] Bualuang, T., Jitsangiam, P., Nusit, K., Rattanasak, U. & Chindaprasirt, P. (2024). Enhancing lateritic soil for sustainable pavement subbase with polymer-modified cement: A comparative study of styrene butadiene rubber and styrene acrylic latex applications. Case Studies in Construction Materials, 21, e03760.
- [29] Shi, C., Wang, P., Ma, C., Zou, X. & Yang, L. (2021). Effects of SAE and SBR on properties of rapid hardening repair mortar. Journal of Building Engineering, 35, 102000.
- [30] Jambeck, J.R. and Walker-Franklin, I., 2023. The impacts of plastics' life cycle. One Earth, 6(6), pp.600-606.

- [31] Silvestre, J.D., De Brito, J. and Pinheiro, M.D., 2011, May. Life-cycle assessment of thermal insulation materials for external walls of buildings. In Proceedings international conference of constructions, Innsbruck.
- [32] Joensuu, T., Leino, R., Heinonen, J. and Saari, A., 2022. Developing Buildings' Life Cycle Assessment in Circular Economy-Comparing methods for assessing carbon footprint of reusable components. Sustainable Cities and Society, 77, p.103499.
- [33] Environment, U.N., Scrivener, K.L., John, V.M. and Gartner, E.M., 2018. Ecoefficient cements: Potential economically viable solutions for a low-CO2 cement-based materials industry. Cement and concrete Research, 114, pp.2-26.
- [34] Ohama, Y., 1998. Polymer-based admixtures. Cement and concrete composites, 20(2-3), pp.189-212.
- [35] Bhutta, M.A.R., Ohama, Y. and Tsuruta, K., 2011. Strength properties of polymer mortar panels using methyl methacrylate solution of waste expanded polystyrene as binder. Construction and building materials, 25(2), pp.779-784.
- [36] Eskander, S.B., Saleh, H.M., Tawfik, M.E. and Bayoumi, T.A., 2021. Towards potential applications of cement-polymer composites based on recycled polystyrene foam wastes on construction fields: Impact of exposure to water ecologies. Case Studies in Construction Materials, 15, p.e00664.
- [37] Osemeahon, S.A., Barminas, J.T. & Jang, A.L. (2013) Development of Waste Polystyrene as a Binder for Emulsion Paint Formulation I: Effect of Polystyrene Concentration. The International Journal of Engineering and Science, 2(8), 30–35.
- [38] Yang, F., Tchekwagep, J.J.K., Wang, S., Huang, S. and Cheng, X., 2024. The effect of extensive heat exposure on the mechanical properties of polymer-modified sulfoaluminate cement repair mortar. Case Studies in Construction Materials, 20, p.e03348.
- [39] Kioupis, D., Skaropoulou, A., Tsivilis, S. and Kakali, G., 2022. Properties and durability performance of lightweight fly ash based geopolymer composites incorporating expanded polystyrene and expanded perlite. Ceramics, 5(4), pp.821-836.
- [40] Sha, W. and Pereira, G.B., 2001. Differential scanning calorimetry study of ordinary Portland cement paste containing metakaolin and theoretical approach of metakaolin activity. Cement and Concrete Composites, 23(6), pp.455-461.
- [41] Samper, M.D., Garcia-Sanoguera, D., Parres, F. and López, J., 2010. Recycling of expanded polystyrene from packaging. Progress in Rubber Plastics and Recycling Technology, 26(2), pp.83-92.
- [42] Athukorala, N., Jayasinghe, M.T.R. and Shea, A., 2025. Thermal characteristics of commercially manufactured expanded polystyrene composite lightweight concrete. Next Materials, 8, p.100854.
- [43] Aattache, A. (2023). Effect of high temperature on polymer-modified mortars using the plastic waste of polyethylene as reinforcement. Journal of Building Engineering, 77, 107498.
- [44] Fediuk, R., Amran, M., Vatin, N., Vasilev, Y., Lesovik, V. & Ozbakkaloglu, T. (2021). Acoustic properties of innovative concretes: A review. Materials, 14(2), 398.
- [45] Amran, M., Fediuk, R., Murali, G., Vatin, N. & Al-Fakih, A. (2021). Sound-absorbing acoustic concretes: A review. Sustainability, 13(19), 10712.
- [46] Zhang, Y.H., Wang, H., Zhong, W.L. and Fan, L.F., 2024. Development of a high-strength lightweight geopolymer concrete for structural and thermal insulation applications. Case Studies in Construction Materials, 21, p.e03949.
- [47] Park, J.K. and Kim, M.O., 2020. Mechanical properties of cement-based materials with recycled plastic: a review. Sustainability, 12(21), p.9060.

- [48] Farinha, C.B., Jankovic, J. and Veiga, M.D.R., 2021. Eco-efficient rendering mortars: use of recycled materials. Woodhead Publishing.
- [49] Kim, H.K. and Lee, H.K., 2010. Acoustic absorption modeling of porous concrete considering the gradation and shape of aggregates and void ratio. Journal of Sound and Vibration, 329(7), pp.866-879.